

An Experimentally Observed Trimetallofullerene $\text{Sm}_3@I_h\text{-C}_{80}$: Encapsulation of Three Metal Atoms in a Cage without a Nonmetallic Mediator

Wei Xu,^{†,⊥} Lai Feng,^{*,‡,⊥} Matteo Calvaresi,[§] Jia Liu,[†] Yang Liu,[†] Ben Niu,^{||} Zujin Shi,^{*,†} Yongfu Lian,^{||} and Francesco Zerbetto^{*,§}

[†]Beijing National Laboratory for Molecular Sciences, State Key Laboratory of Rare Earth Materials Chemistry and Applications, College of Chemistry and Molecular Engineering, Peking University, Beijing 100871, P. R. China

[‡]Jiangsu Key Laboratory of Thin Films and School of Energy, Soochow University, Suzhou 215006, P. R. China

[§]Dipartimento di Chimica "G. Ciamician", Università di Bologna, Via F. Selmi 2, 40126 Bologna, Italy

^{||}School of Chemistry and Materials Science, Heilongjiang University, Harbin 150080, P. R. China

Supporting Information

ABSTRACT: We report the synthesis, isolation, and characterizations of the novel trimetallofullerene $\text{Sm}_3@I_h\text{-C}_{80}$. Importantly, the experimental X-ray structure of $\text{Sm}_3@I_h\text{-C}_{80}$ verified for the first time that three metal atoms can be stabilized in a fullerene cage without a nonmetal mediator. Furthermore, computational studies demonstrated the electronic features of $\text{Sm}_3@I_h\text{-C}_{80}$, which are similar to that of theoretically studied $\text{Y}_3@I_h\text{-C}_{80}$. Electrochemical studies of $\text{Sm}_3@I_h\text{-C}_{80}$ showed a major difference from those of the well-studied isoelectronic species $\text{Sc}_3\text{N}@I_h\text{-C}_{80}$ and $\text{La}_2@I_h\text{-C}_{80}$.

Fullerenes that encapsulate metal atoms or metallic clusters in their cage cavities have been termed endohedral metallofullerenes (EMFs). Such species are fascinating because of their tunable chemical, electrochemical, and physical properties, which are highly related to their endohedral compositions.¹ Accordingly, many studies aimed at exploring new EMFs have been performed with a focus on the variety of endohedral clusters.^{2–6} Hopefully, such efforts can provide opportunities to develop novel conductors,⁷ magnets,⁸ and building blocks of photosynthetic or photovoltaic systems.⁹

Conventional EMFs containing one or two metal atoms were discovered in the early years.^{1a} More recent studies revealed that fullerene cages can also encapsulate large clusters, including metal nitride (M_3N),³ metal carbide ($\text{M}_{2,3,4}\text{C}_2$),² metal oxide ($\text{Sc}_{2,4}\text{O}_{1,2,3}$),⁴ metal sulfide (Sc_2S),⁵ and metal cyanide (Sc_3CN) clusters.⁶ To the best of our knowledge, encapsulation of three or more metal atoms has been achieved only by doping with nonmetal atoms. It appears that the nonmetal atoms can mediate or stabilize the multiply trapped metal atoms by interacting with them. Furthermore, such a proposal has been confirmed by density functional theory (DFT) calculations. Detailed theoretical analysis revealed that the intracage bonding in nitride- and carbide-cluster fullerenes exhibits a high degree of covalency.¹⁰ Thus, the question of whether it is possible to encapsulate three metal atoms in a fullerene cage in the form of trimetallic (M_3) cluster

arises. However, past answers are ambiguous. In early studies, Er_3C_{74} ,¹¹ Tb_3C_{80} ,¹² and Dy_3C_{98} ¹³ were analyzed via only mass spectrometry (MS) or UV–vis or FTIR spectroscopy. Recently, the long-believed $\text{Sc}_3@C_{82}$ was proved to be the carbide-cluster fullerene $\text{Sc}_3\text{C}_2@C_{80}$.^{2b} More definitely, the formation of $\text{Y}_3@I_h\text{-C}_{80}$ was reported through a combined DFT/MS study.¹⁴ Nevertheless, because of the lack of further structural characterization by NMR spectroscopy or X-ray diffraction (XRD), $\text{M}_3@C_{2n}$ species, especially their structures, to date remain unconfirmed from an experimental perspective.

Here we report for the first time the synthesis, isolation, and experimental characterization of a trimetallofullerene, $\text{Sm}_3@I_h\text{-C}_{80}$. Specifically, the Sm_3 cluster encapsulated in the $I_h\text{-C}_{80}$ cage was unambiguously identified using single-crystal XRD, thus ruling out the possibility that Sm_3C_{80} is actually the carbide-cluster species $\text{Sm}_3\text{C}_2@C_{78}$. Furthermore, the electronic features of $\text{Sm}_3@I_h\text{-C}_{80}$ were investigated via DFT calculations and electrochemical studies.

The synthesis and isolation of Sm_3C_{80} are described in the Supporting Information (see Figures S1–S4). Because of the low yield of Sm_3C_{80} , only ca. 0.5 mg of sample was obtained during a work period of 7 months. The absolute structure of $\text{Sm}_3@I_h\text{-C}_{80}$ was unambiguously determined by XRD. Cocrystals of $\text{Sm}_3@I_h\text{-C}_{80}/[\text{Ni}^{\text{II}}(\text{OEP})]$ (OEP = octaethylporphyrin) were obtained using a diffusion method. The molecular structure was resolved and refined in the $C2/m$ space group. Figure 1 shows the X-ray structure of $\text{Sm}_3@I_h\text{-C}_{80}$ together with an adjacent $[\text{Ni}^{\text{II}}(\text{OEP})]$ moiety. The $I_h\text{-C}_{80}$ cage disordered over two orientations with occupancies of 0.34 and 0.16. Inside the cage, multiple partially occupied Sm sites were identified. Figure S5 shows the major set of Sm sites as well as all of the other Sm sites, including those generated by the crystallographic mirror plane. One of the major Sm sites (i.e., Sm1), with a fractional occupancy of 0.312 versus the cage occupancy of 0.50, resides on the crystallographic mirror plane and is far from the porphyrin moiety. Two other major Sm sites (i.e., Sm2 and Sm3A), each with a refined fractional occupancy

Received: November 23, 2012

Published: March 6, 2013

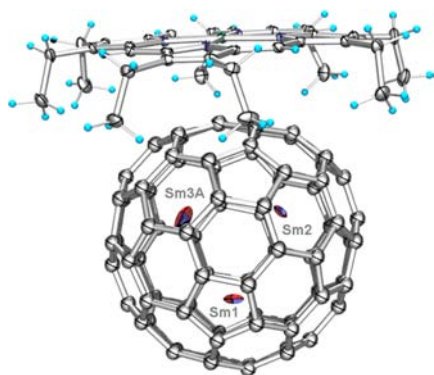


Figure 1. ORTEP drawing of $\text{Sm}_3@I_h\text{-C}_{80}\cdot\text{Ni}^{\text{II}}(\text{OEP})$ with 35% thermal ellipsoids, showing the intermolecular interaction. The major cage position with fractional occupancy of 0.34 and the major Sm sites are depicted. Solvent molecules have been omitted for clarity.

of 0.311, are situated in close proximity to the porphyrin moiety. Thus, these three major Sm sites have similar occupancies and form a triangle with Sm–Sm distances ranging from 3.173 to 3.313 Å, which are much shorter than those in $\text{Sc}_3\text{N}@I_h\text{-C}_{80}$ ($d_{\text{Sc-Sc}} = 3.490\text{--}3.510$ Å)¹⁵ and $\text{Gd}_3\text{N}@I_h\text{-C}_{80}$ ($d_{\text{Gd-Gd}} = 3.409\text{--}3.449$ Å).¹⁶ It should be noted that the common oxidation state of Sm in this EMF is 2+. The ionic radius of Sm^{2+} (1.14 Å) is larger than that of Sc^{3+} (0.88 Å) and comparable to that of Gd^{3+} (1.08 Å). However, the volume of the Sm_3 cluster is somewhat smaller than that of either Sc_3N or Gd_3N , which may be readily explained by the absence of a central nonmetal atom in the Sm_3 cluster.

Moreover, if the major cage position is taken into consideration, the Sm1 and Sm2 sites both reside under hexagonal rings with metal-to-ring-centroid distances of 2.108 and 2.136 Å, respectively, whereas Sm3A is close to a 6,6-bond with a metal-to-bond distance of 2.247 Å. The average distance from the major Sm sites to the nearest cage carbons is ca. 2.4 Å (Figure S6), which is similar to the Gd–C distance in $\text{Gd}_3\text{N}@I_h\text{-C}_{80}$ (2.344–2.439 Å). Because of the similar ionic radii of Sm^{2+} and Gd^{3+} , these similar metal-to-cage-carbon distances might reflect comparable cage–cluster interactions in $\text{Sm}_3@I_h\text{-C}_{80}$ and $\text{Gd}_3\text{N}@I_h\text{-C}_{80}$, despite their different cluster compositions.

Apart from the major Sm sites, several minor Sm sites with fractional occupancies ranging from 0.087 to 0.015 were found inside the cage (Figure S5). Most of them are distributed around or between the Sm2/Sm2A and Sm3A/Sm3 sites, indicating the two-dimensional movement of the two Sm atoms that are close to the porphyrin moiety. In contrast, the other Sm atom appears to be more localized, as only two minor Sm sites (i.e., Sm4 and Sm10) are present in the vicinity of the Sm1 site. The sum of the occupancies of all of these Sm sites is 1.38, which is nearly three times larger than the cage occupancy (i.e., 0.5). Also, additional electron density remained in the cage and could not be modeled during refinement, indicating the rotation state of the Sm_3 cluster.

Furthermore, the composition of Sm_3C_{80} was confirmed by matrix-assisted laser desorption/ionization time of flight (MALDI-TOF) MS. As shown in Figure 2, a single mass peak was observed at m/z 1413, and the isotopic distribution agreed well with the theoretical calculation for Sm_3C_{80} . In addition, $\text{Sm}_3@C_{80}$ displayed a featureless absorption in the 400–1600 nm range in either CS_2 or toluene solution, similar to $\text{M}_2@I_h\text{-C}_{80}$ ($M = \text{La}, \text{Ce}$).^{17a} On the other hand, the

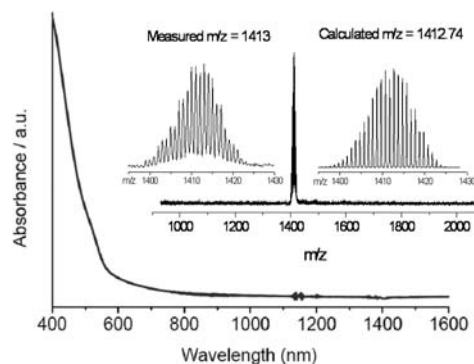


Figure 2. UV–vis–NIR spectrum of isolated Sm_3C_{80} dissolved in toluene. The inset shows the positive-ion MALDI-TOF mass spectrum of Sm_3C_{80} with measured and calculated isotopic distributions.

characteristic absorption of $\text{M}_2@D_{5h}\text{-C}_{80}$ ($M = \text{La}, \text{Ce}$),^{17b} which appears at 467 nm, was not seen for $\text{Sm}_3@C_{80}$. Thus, the spectral study might suggest I_h rather than D_{5h} cage symmetry for $\text{Sm}_3@C_{80}$, consistent with the XRD results. Notably, the spectral onset of Sm_3C_{80} is at ca. 900 nm (Figure S4), a longer wavelength than that of $\text{Sc}_3\text{N}@I_h\text{-C}_{80}$, which indicates a lower band gap in $\text{Sm}_3@C_{80}$.

To investigate the electronic features of $\text{Sm}_3@I_h\text{-C}_{80}$, DFT calculations were performed, starting from the crystal structure. The highest occupied molecular orbital (HOMO) of $\text{Sm}_3@I_h\text{-C}_{80}$ (Figure 3a) is mainly localized on the cage, with small Sm

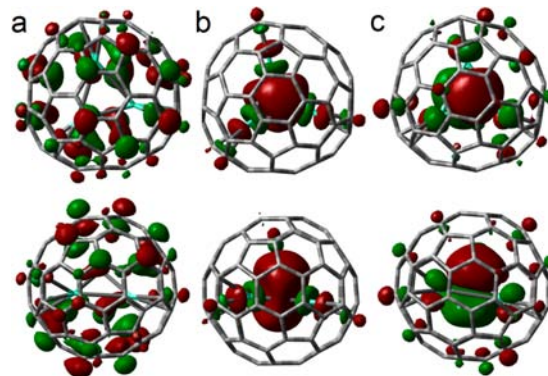


Figure 3. (top) Front and (bottom) side views of MOs of $\text{Sm}_3@I_h\text{-C}_{80}$: (a) HOMO (−5.88 eV); (b) LUMO (−3.79 eV); (c) LUMO+1 (−3.47 eV). The LUMO and LUMO+1 resemble the s-like and p-like orbitals of the pseudoatom.

contributions. In contrast, the lowest occupied MO (LUMO) is centered on the endohedral Sm cluster, forming orbitals similar to the “interstitial” orbitals known for metal clusters, as described previously by McAdon and Goddard¹⁸ and Popov et al.¹⁴ for EMFs. The non-nuclear attractor (NNA) (i.e., the maximum of the electron density, also called the “pseudoatom”) is at the center of the cage, and each Sm atom forms a bond with it. The NNA of $\text{Sm}_3@C_{80}$, as in the case of $\text{Y}_3@C_{80}$, mimics the effect of the nonmetal atom that normally mediates or stabilizes multiple trapped metal atoms. Comparison of the frontier MOs of $\text{Sm}_3@C_{80}$ and $\text{Y}_3@C_{80}$ shows that they resemble each other and follow the same aufbau principle. However, because of the existence of an unpaired electron on the Y atom, in $\text{Y}_3@C_{80}$ there is a singly occupied MO that corresponds to the LUMO of $\text{Sm}_3@C_{80}$. The peculiar

properties of $\text{Sm}_3@C_{80}$ stem from the fact that all of the metal-centered MOs are unoccupied.

The calculated Mulliken charges of the Sm atoms are 1.12, 1.12 and 1.17, and the cluster charge is -3.41 . These values are in line with the results of similar calculations on $\text{Sc}_3\text{N}@C_{80}$ and $\text{Y}_3@C_{80}$ ¹⁹ and imply a formal transfer of six electrons from the cluster to the cage with subsequent coordination of the Sm cations to the cage as “ligands”, with concomitant reoccupation of Sm atomic orbitals (AOs). Analysis showed that there are no specific AOs that are responsible for the cage-to-cluster electron back-transfer. Instead, the interaction occurs from many cage orbitals to Sm AOs.

Further calculations of the charge and spin distributions in $\text{Sm}_3@C_{80}^-$ (Figure 4b) revealed an interesting peculiarity of its

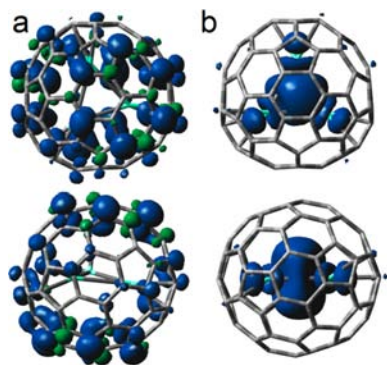


Figure 4. (top) Front and (bottom) side views of the spin densities for (a) oxidized and (b) reduced $\text{Sm}_3@I_h\text{-C}_{80}$.

electronic structure: while the unpaired spin density mostly resides on the endohedral cluster, the cluster charge decrease only slightly to 3.11. Popov and Dunsch¹⁹ previously suggested the possibility of spatial charge–spin separation in all endohedral fullerenes, with a high contribution of metal atom orbitals to the LUMO. The addition of an electron to $\text{Sm}_3@C_{80}$ formally increases the population of the Sm orbitals. Simultaneously, it also decreases the back-donation. The net result is that (i) the overall Sm orbital population and therefore charge are not significantly altered, (ii) the negative charge is delocalized over the cage, and (iii) the spin of $\text{Sm}_3@C_{80}^-$ resides on the cluster to the same degree that the LUMO is localized on it. On the contrary, oxidation involves only cage contributions: spin and charge changes are entirely localized on the cage, without any involvement of the endohedral cluster (Figure 4a). Interestingly, full geometry optimization showed that while oxidation does not perturb the geometry of the system, reduction triggers a conformational rearrangement of the cluster, as also found by Popov and Dunsch.¹⁹

The electrochemical properties of $\text{Sm}_3@I_h\text{-C}_{80}$ were investigated by means of cyclic voltammetry (CV) and differential pulse voltammetry (DPV). The CV and DPV profiles suggest two one-electron reduction steps on the cathodic side and two one-electron oxidation steps on the anodic side (Figure S7). The redox potentials obtained from CV are summarized in Table 1 and compared with those of other isoelectronic species. Remarkably, the first oxidation potential of $\text{Sm}_3@I_h\text{-C}_{80}$ is much lower than those of $\text{Sc}_3\text{N}@C_{80}$ ²⁰ and $\text{La}_2@C_{80}$,^{17a} indicating a strong electron-donating property. The first reduction potential of $\text{Sm}_3@I_h\text{-C}_{80}$ is also lower than that of $\text{Sc}_3\text{N}@C_{80}$ but higher than that of $\text{La}_2@C_{80}$, suggesting a moderate electron-accepting ability. Moreover, the

Table 1. Redox Potentials of $\text{X}@I_h\text{-C}_{80}$ EMFs^a

X	E_2^{ox}	E_1^{ox}	E_1^{red}	E_2^{red}	E_3^{red}	ΔE^b
Sm_3	0.78	0.30	-0.83	$-1.88^{c,d}$	–	1.13
Sc_3N^e	–	0.62	-1.22^c	-1.59^c	-1.90^e	1.84
La_2^f	–	0.56	-0.31	-1.72	-2.13	0.87

^aAll values are in V vs $\text{Fc}^{0/+}$. Redox potentials are half-cell potentials, unless otherwise noted. ^b $\Delta E = E_1^{\text{ox}} - E_1^{\text{red}}$. ^cIrreversible redox process. ^dDPV value. ^eData taken from ref 20. ^fData taken from ref 17a.

two oxidation steps and the first reduction step of $\text{Sm}_3@I_h\text{-C}_{80}$ are fully reversible, whereas the second reduction step is irreversible at a scan rate of 100, 800 or even 1500 mV s^{-1} (Figure S8). The electrochemical potential gap of $\text{Sm}_3@I_h\text{-C}_{80}$ is 1.13 V, which is substantially smaller than those of most $\text{M}_3\text{N}@I_h\text{-C}_{80}$ EMFs²¹ but a little larger than that of $\text{La}_2@I_h\text{-C}_{80}$. This comparison study therefore shows that the endohedral cluster composition indeed has a significant effect on the electrochemical behavior of EMFs. In addition, despite the small potential gap, which reflects a low band gap in $\text{Sm}_3@I_h\text{-C}_{80}$, this species shows good stability, as no decomposition or oxidation was detected after storage under air for at least 1 month.

In summary, the novel trimetallofullerene $\text{Sm}_3@I_h\text{-C}_{80}$ has been synthesized, isolated, and characterized. Importantly, the structure of the trimetallofullerene has been experimentally observed for the first time by means of XRD, verifying that three metal atoms can be stabilized in a fullerene cage without any involvement of a nonmetal mediator. Furthermore, related DFT calculations showed that the electronic structure of $\text{Sm}_3@I_h\text{-C}_{80}$ features a pseudoatom at the center of the cage and is similar to that of theoretically studied $\text{Y}_3@I_h\text{-C}_{80}$. Electrochemical studies of $\text{Sm}_3@I_h\text{-C}_{80}$ showed a remarkable difference from those of isoelectronic species, including $\text{Sc}_3\text{N}@C_{80}$ and $\text{La}_2@C_{80}$, suggesting a cluster-induced effect on the electrochemical behavior of EMFs.

■ ASSOCIATED CONTENT

📄 Supporting Information

Experiments details and crystallographic data (CIF) for $\text{Sm}_3@I_h\text{-C}_{80}\text{-Ni}^{\text{II}}(\text{OEP})$. This material is available free of charge via the Internet at <http://pubs.acs.org>.

■ AUTHOR INFORMATION

Corresponding Author

fenglai@suda.edu.cn; zjshi@pku.edu.cn; francesco.zerbetto@unibo.it

Author Contributions

[†]W.X. and L.F. contributed equally.

Notes

The authors declare no competing financial interest.

■ ACKNOWLEDGMENTS

This work was supported by the Ministry of Science and Technology of China (2013CB933402, 2011CB932601), the National Natural Science Foundation of China (21171013, 21241004), and the Natural Science Foundation of Jiangsu Province (BK2012611). Also, we are grateful to Prof. T. Akasaka and Dr. M. Suzuki (University of Tsukuba) for their support in the XRD measurements.

■ REFERENCES

- (1) (a) Akasaka, T.; Nagase, S. *Endofullerenes: A New Family of Carbon Clusters*; Kluwer: Dordrecht, The Netherlands, 2002. (b) Feng, L.; Akasaka, T.; Nagase, S. In *Carbon Nanotubes and Related Structures*; Guldi, D. M., Martin, N., Eds.; Wiley-VCH: Weinheim, Germany, 2010; pp 455–490. (c) Lu, X.; Akasaka, T.; Nagase, S. *Chem. Commun.* **2011**, 47, 5942. (d) Lu, X.; Feng, L.; Akasaka, T.; Nagase, S. *Chem. Soc. Rev.* **2012**, 41, 7723.
- (2) (a) Wang, C. R.; Kai, T.; Tomiyama, T.; Yoshida, T.; Kobayashi, Y.; Nishibori, E.; Takata, M.; Sakata, M.; Shinohara, H. *Angew. Chem., Int. Ed.* **2001**, 40, 397. (b) Iiduka, Y.; Wakahara, T.; Nakahodo, T.; Tsuchiya, T.; Sakuraba, A.; Maeda, Y.; Akasaka, T.; Yoza, K.; Horn, E.; Kato, T.; Liu, M. T. H.; Mizorogi, N.; Kobayashi, K.; Nagase, S. *J. Am. Chem. Soc.* **2005**, 127, 12500. (c) Iiduka, Y.; Wakahara, T.; Nakajima, K.; Nakahodo, T.; Tsuchiya, T.; Maeda, Y.; Akasaka, T.; Yoza, K.; Liu, M. T. H.; Mizorogi, N.; Nagase, S. *Angew. Chem., Int. Ed.* **2007**, 46, 5562. (d) Yamazaki, Y.; Nakajima, K.; Wakahara, T.; Tsuchiya, T.; Ishitsuka, M. O.; Maeda, Y.; Akasaka, T.; Waelchli, M.; Mizorogi, N.; Nagase, S. *Angew. Chem., Int. Ed.* **2008**, 47, 7905. (e) Kurihara, H.; Lu, X.; Iiduka, Y.; Mizorogi, N.; Slanina, Z.; Tsuchiya, T.; Akasaka, T.; Nagase, S. *J. Am. Chem. Soc.* **2011**, 133, 2382. (f) Lu, X.; Nakajima, K.; Iiduka, Y.; Nikawa, H.; Mizorogi, N.; Slanina, Z.; Tsuchiya, T.; Nagase, S.; Akasaka, T. *J. Am. Chem. Soc.* **2011**, 133, 19553. (g) Lu, X.; Nakajima, K.; Iiduka, Y.; Nikawa, H.; Tsuchiya, T.; Mizorogi, N.; Slanina, Z.; Nagase, S.; Akasaka, T. *Angew. Chem., Int. Ed.* **2012**, 51, 5889.
- (3) (a) Stevenson, S.; Rice, G.; Glass, T.; Harich, K.; Cromer, F.; Jordan, M. R.; Craft, J.; Hadju, E.; Bible, R.; Olmstead, M. M.; Maitra, K.; Fisher, A. J.; Balch, A. L.; Dorn, H. C. *Nature* **1999**, 401, 55. (b) Zuo, T. M.; Beavers, C. M.; Duchamp, J. C.; Campbell, A.; Dorn, H. C.; Olmstead, M. M.; Balch, A. L. *J. Am. Chem. Soc.* **2007**, 129, 2035. (c) Beavers, C. M.; Chaur, M. N.; Olmstead, M. M.; Echegoyen, L.; Balch, A. L. *J. Am. Chem. Soc.* **2009**, 131, 11519.
- (4) (a) Stevenson, S.; Mackey, M. A.; Stuart, M. A.; Phillips, J. P.; Easterling, M. L.; Chancellor, C. J.; Olmstead, M. M.; Balch, A. L. *J. Am. Chem. Soc.* **2008**, 130, 11844. (b) Mercado, B. Q.; Stuart, M. A.; Mackey, M. A.; Pickens, J. E.; Confait, S. B.; Stevenson, S.; Easterling, M. L.; Valencia, R.; Rodríguez-Fortea, A.; Poblet, J. M.; Olmstead, M. M.; Balch, A. L. *J. Am. Chem. Soc.* **2010**, 132, 12098.
- (5) (a) Chen, N.; Beavers, C. M.; Mulet-Gas, M.; Rodríguez-Fortea, A.; Munoz, E. J.; Li, Y.-Y.; Olmstead, M. M.; Balch, A. L.; Poblet, J. M.; Echegoyen, L. *J. Am. Chem. Soc.* **2012**, 134, 7851. (b) Mercado, B. Q.; Chen, N.; Rodríguez-Fortea, A.; Mackey, M. A.; Stevenson, S.; Echegoyen, L.; Poblet, J. M.; Olmstead, M. M.; Balch, A. L. *J. Am. Chem. Soc.* **2011**, 133, 6752. (c) Dunsch, L.; Yang, S.; Zhang, L.; Svitova, A.; Oswald, S.; Popov, A. A. *J. Am. Chem. Soc.* **2010**, 132, 5413.
- (6) Wang, T. S.; Feng, L.; Wu, J. Y.; Xu, W.; Xiang, J. F.; Tan, K.; Ma, Y. H.; Zheng, J. P.; Jiang, L.; Lu, X.; Shu, C. Y.; Wang, C. R. *J. Am. Chem. Soc.* **2010**, 132, 16362.
- (7) (a) Sato, S.; Nikawa, H.; Seki, S.; Wang, L.; Luo, G.; Lu, J.; Haranaka, M.; Tsuchiya, T.; Nagase, S.; Akasaka, T. *Angew. Chem., Int. Ed.* **2012**, 51, 1. (b) Sato, S.; Seki, S.; Honsho, Y.; Wang, L.; Nikawa, H.; Luo, G.; Lu, J.; Haranaka, M.; Tsuchiya, T.; Nagase, S.; Akasaka, T. *J. Am. Chem. Soc.* **2011**, 133, 2766. (c) Tsuchiya, T.; Kumashiro, R.; Tanigaki, K.; Matsunaga, Y.; Ishitsuka, M. O.; Wakahara, T.; Maeda, Y.; Takano, Y.; Aoyagi, M.; Akasaka, T.; Liu, M. T. H.; Kato, T.; Suenaga, K.; Jeong, J. S.; Iijima, S.; Kimura, F.; Kimura, T.; Nagase, S. *J. Am. Chem. Soc.* **2008**, 130, 450. (d) Kobayashi, S.; Mori, S.; Iida, S.; Ando, H.; Takenobu, T.; Taguchi, Y.; Fujiwara, A.; Taninaka, A.; Shinohara, H.; Iwasa, Y. *J. Am. Chem. Soc.* **2003**, 125, 8116.
- (8) Westerström, R.; Dreiser, J.; Piamonteze, C.; Muntwiler, M.; Weyeneth, S.; Brune, H.; Rusponi, S.; Nolting, F.; Popov, A. A.; Yang, S.; Dunsch, L.; Greber, T. *J. Am. Chem. Soc.* **2012**, 134, 9840.
- (9) (a) Ross, R. B.; Cardona, C. M.; Guldi, D. M.; Sankaranarayanan, S. G.; Reese, M. O.; Kopidakis, N.; Peet, J.; Walker, B.; Bazan, G. C.; Van Keuren, E.; Holloway, B. C.; Drees, M. *Nat. Mater.* **2009**, 8, 208. (b) Feng, L.; Slanina, Z.; Sato, S.; Yoza, K.; Tsuchiya, T.; Mizorogi, N.; Akasaka, T.; Nagase, S.; Martin, N.; Guldi, D. M. *Angew. Chem., Int. Ed.* **2011**, 50, 5909. (c) Feng, L.; Radhakrishnan, S. G.; Mizorogi, N.; Slanina, Z.; Nikawa, H.; Tsuchiya, T.; Akasaka, T.; Nagase, S.; Martin, N.; Guldi, D. M. *J. Am. Chem. Soc.* **2011**, 133, 7608. (d) Rudolf, M.; Wolfrum, S.; Guldi, D. M.; Feng, L.; Tsuchiya, T.; Akasaka, T.; Echegoyen, L. *Chem.—Eur. J.* **2012**, 18, 5136. (e) Feng, L.; Rudolf, M.; Wolfrum, S.; Troeger, A.; Slanina, Z.; Akasaka, T.; Nagase, S.; Martin, N.; Ameri, T.; Brabec, C. J.; Guldi, D. M. *J. Am. Chem. Soc.* **2012**, 134, 12190.
- (10) Popov, A. A.; Dunsch, L. *Chem.—Eur. J.* **2009**, 15, 9707.
- (11) Tagmatarchis, N.; Aslanis, E.; Prassides, K.; Shinohara, H. *Chem. Mater.* **2001**, 13, 2374.
- (12) Lian, Y. F.; Shi, Z. J.; Zhou, X. H.; Gu, Z. N. *Chem. Mater.* **2004**, 16, 1704.
- (13) Yang, S. F.; Dunsch, L. *Angew. Chem., Int. Ed.* **2006**, 45, 1299.
- (14) Popov, A. A.; Zhang, L.; Dunsch, L. *ACS Nano* **2010**, 4, 795.
- (15) Stevenson, S.; Lee, H. M.; Olmstead, M. M.; Kozikowski, C.; Stevenson, P.; Balch, A. L. *Chem.—Eur. J.* **2002**, 8, 4528.
- (16) Stevenson, S.; Phillips, J. P.; Reid, J. E.; Olmstead, M. M.; Rath, S. P.; Balch, A. L. *Chem. Commun.* **2004**, 2814.
- (17) (a) Suzuki, T.; Maruyama, Y.; Kato, T.; Kikuchi, K.; Nakao, Y.; Achiba, Y.; Kobayashi, K.; Nagase, S. *Angew. Chem., Int. Ed. Engl.* **1995**, 34, 1094. (b) Yamada, M.; Mizorogi, N.; Tsuchiya, T.; Akasaka, T.; Nagase, S. *Chem.—Eur. J.* **2009**, 15, 9486.
- (18) McAdon, M. H.; Goddard, W. A., III. *Phys. Rev. Lett.* **1985**, 55, 2563.
- (19) Popov, A. A.; Dunsch, L. *J. Am. Chem. Soc.* **2008**, 130, 17726.
- (20) Iiduka, Y.; Ikenaga, O.; Sakuraba, A.; Wakahara, T.; Tsuchiya, T.; Maeda, Y.; Nakahodo, T.; Akasaka, T.; Kako, M.; Mizorogi, N.; Nagase, S. *J. Am. Chem. Soc.* **2005**, 127, 9956.
- (21) Chaur, M. N.; Melin, F.; Ortiz, A. L.; Echegoyen, L. *Angew. Chem., Int. Ed.* **2009**, 48, 7514.